LARGE-SCALE EXPERIMENT ON DYNAMIC RESPONSE OF SAND BED AROUND A CYLINDER DUE TO TSUNAMI

by

Fuminori KATO[1], Shinji SATO[2] and Harry YEH[3]

ABSTRACT

The scour process around a vertical cylinder due to tsunami runup was investigated experimentally using the large-scale tsunami facility at Public Works Research Institute. Scouring around a cylinder during tsunami runup was optically observed with the multiple CCD cameras that were installed inside of the cylinder. All the other necessary information, e.g. water depth, flow velocity and pore pressure, were obtained by the conventional electronic sensors. In addition, we measured the topography changes before and after the tsunami runup. The temporal variations of the scour process were clarified. The correlations between scouring, wave height, water volume of runup and liquefaction were also discussed.

KEY WORDS: Liquefaction
Runup
Scouring
Tsunami

1. INTRODUCTION

It is well known that a tsunami attack causes substantial erosion and scour on the shore. For example, the 1960 Chilean tsunami scoured out the port entrance by more than 10 m at Kesen-numa Port in Japan. Several tsunami surveys, from the 1992 Nicaragua tsunami to the 1998 Papua New Guinea tsunami, also discovered substantial tsunami scouring effects around structures and trees. In fact, scouring is sometimes the primary cause of structure damage and destruction. There are a variety of structures exist in coastal zones, such as straight-line structures like revetments and cylindrical shape structures like oil tanks.

It is likely that the scouring around on-shore structures caused by tsunami runup is different from the present understanding of sediment transport and bridge-pier-type scour processes in river and coastal environments. Flows associated with tsunami runup are far from being steady or uniform, and the scouring takes place over a short duration, often less than fifteen minutes. It is also important to comprehend the onshore conditions during tsunami runup, where soils (sediments) are initially not fully saturated and suddenly become wet on the surface while the majority of pore spaces are still filled with air. This complex and important problem must first be approached experimentally to understand the physics and mechanisms of scour phenomena associated with tsunami runup. Because of the importance of the scale effects expected in sediment motion, the laboratory experiments must be performed in a sufficiently large experimental facility.

The previous investigation of tsunami scouring processes is limited. Uda et al. (1987) found that scouring near a revetment due to tsunamis is governed by topography behind a revetment. As for scouring in front of a revetment, Nishimura and Horikawa (1979) and Noguchi et al. (1997) identified some correlation between scour depth and water depth in front of a revetment for tsunami drawdown processes.

---

1) Research Engineer, Coast Division, Public Works Research Institute, Asahi 1, Tsukuba-shi, Ibaraki-ken, 305-0804, Japan

2) Former Head, ditto

3) Professor, Department of Civil and Environmental Engineering, University of Washington, Box 352700, Seattle, Washington 98195-2700, U.S.A.

2. EXPERIMENT CONDITION

A series of experiments was performed in a 135 m long, 2 m wide, 5 m deep sediment tank at Public Works Research Institute, Tsukuba, Japan. To generate a wide variety of long waves, the tank is equipped with a piston-type wave-maker driven by the large servo motor. The maximum stroke of the wave paddle is 2.4 m with the maximum speed of 1.11 m/s. It was tested and proven to generate a clean solitary wave of at least 40 cm high in a 3 m water depth. A beach of well-graded sediment (approximately D_{50} = 0.35 mm sand particles) was constructed with a uniform slope of 1/20. A model cylinder was placed upright on the beach. The cylinder is 50 cm in diameter, made of 1 cm thick Plexiglas, water tight at the bottom end, and connected above to an aluminum cylinder in order to assure its stiffness. Because of the transparent cylinder wall, the scour process can be recorded from the interior with three miniature CCD video cameras, which cover more than 180-degree view of the circumference from the upstream to the downstream sides. Wave gages, an electromagnetic flow meter and pore pressure transducers were placed as shown in Figure 1. In addition, before and after each experiment, topography surveys were conducted in the 4 m by 1 m region around the cylinder.

The experiments were performed for total 11 cases as listed in Table 1. Note that the last two cases in Table 1 are those for a plane beach without placing the cylinder. The nonlinearity of an incident solitary wave was parameterized by the ratio (a/h) of wave height a to offshore water depth h. Three different incident wave conditions were used in terms of the nonlinear parameter a/h = 0.13 (cases 1, 2 and 3), 0.09 (cases 4, 5, and 6), and 0.05 (cases 7, 8, and 9). Three different offshore water depths were used: 2.25 m for the case 1, 4 and 7: 2.45 m for the case 2, 5 and 8: 2.65 m for the case 3, 6 and 9. Since the location of the model cylinder is fixed throughout the experiments, the offshore water depth was varied with h = 2.25 m, 2.45 m and 2.65 m, which correspond with the cylinder location at 4 m onshore from the still shoreline, on the shoreline and at 4 m offshore, respectively.

In order to evaluate the effect of existence of the cylinder, the maximum runup heights were measured with and without the cylinder placement using the identical incident wave condition. Under the condition of 2.65 m offshore water depth, the maximum runup height of Case 6 (with the cylinder) is 2 cm lower than Case 10 (without the cylinder). With 2.45 m offshore water depth, the runup of Case 5 (with the cylinder) is 5 cm lower than Case 11 (without the cylinder). These results indicate that the presence of the cylinder reduces the tsunami runup height very slightly. Consequently the blockage of the runup motion by the cylinder is negligible and the tank width is considered wide enough to neglect the side-wall effects.

3. RESULT OF TOPOGRAPHY SURVEY BEFORE AND AFTER TSUNAMI

Before and after each experiment, topography survey was conducted in the area of 1 m wide from the center of the cylinder toward the tank wall, 2 m onshore and 2 m offshore from the center of the cylinder. The measurement interval of 20 cm was used before the experiment, and after the experiment, the finer interval of 5 cm was used within 50 cm from the cylinder, and 10 cm interval beyond 50 cm from the cylinder.

Figure 2 shows beach level changes along the offshore line from the center of the cylinder. The positive values indicate deposition and the negative values indicate scour. The beach level variations were normalized by the initial water depth offshore. The distance from the cylinder was normalized by the tank width. Only for Cases 2 and 5, apparent local scouring resulted in the offshore region from the cylinder.

Figure 3 shows beach level changes along the longshore line from the cylinder. Local scouring

occurred in most cases. The maximum scour depth of 10 cm was found in Case 3 at 10 cm away from the cylinder. The larger the wave height, the deeper the scour depth. Furthermore, for a given incident wave condition, the larger scouring depth appears to result when the cylinder was placed offshore. It is noted that, in the cases where the cylinder was on the shoreline, erosion occurred everywhere along the longshore line.

Figure 4 shows beach level changes along the onshore line from the cylinder. Local scouring was occurred in most cases. The maximum scour depth of 7.7 cm was measured for Case 2 at 5 cm inland from the cylinder. The larger the wave height, the larger the scouring depth. When the cylinder was placed on the shoreline (i.e. Case 2 and 5), resulting scouring was the most severe for a given incident wave condition. In Cases 2 and 5, the erosion was observed as far as 1 m off the cylinder.

Figure 5 shows the relation between incident wave height and scour area of the depth with more than 2 cm deep. The scour area was normalized by the area of the cylinder. The wave height was normalized by the initial water depth offshore. In comparison with the cases when the cylinder was placed inshore on the beach, the scour area was larger when the cylinder was placed on the shoreline or offshore. The scour area appears to be proportional to the wave height; the scour area is much more sensitive to the incident wave height when the cylinder is at the shoreline.

Figure 6 shows the relation between the incident wave height and the sediment volume change in the area near the cylinder. The area of the measurement is 1 m long in the cross-shore direction and 0.5 m wide in the along-shore direction with the one long edge bisecting the cylinder in the cross-shore direction. The volume was normalized by the cylinder area times the initial water depth offshore. The net volume change for the case with the cylinder being placed inshore is smaller than that the other cases; the changes are comparable for the cases of the cylinder on the shoreline and at the offshore location. The proportionality shown in Fig. 6 appears to be similar for all three cases with different locations of the cylinder.

4. SCOUR AROUND A CYLINDER ELUCIDATED BY VIDEO ANALYSIS

To clarify scouring mechanisms around the cylinder, sand response along the cylinder wall was observed with three miniature CCD video cameras installed inside of the cylinder. This can be accomplished due to its large size cylinder model (50 cm in diameter) that is made of a transparent (Plexiglas) cylinder wall.

The sand response at the cylinder wall for Case 3 is shown in Fig. 7. Camera 1 (left column), camera 2 (center column) and camera 3 (right column) cover the views from offshore to side, side direction, and from side to onshore, respectively; each covers more than 90 degrees of the view angle to ensure that obtained images overlap each other with sufficient margins. The images on the top of Fig. 7 represent the condition prior to the tsunami runup, the middle were those at the maximum inundation, and those on the bottom were after the tsunami drawdown. The scour depths of three points (offshore, side and onshore) around the cylinder were determined from these images.

Scour-depth variations at the point facing offshore are shown in Fig. 8. The depths are all normalized by the diameter of the cylinder. During the tsunami runup, scouring resulted in most cases, i.e. the sand-surface elevation decreased. During the drawdown, sand accumulation occurred in the cases with the large scour depth at the maximum inundation. This behavior is evident in the cases with the cylinder located onshore and on the shoreline; especially in case 4, its scour depth at the maximum inundation is five times as large as that just after tsunami drawdown. At the maximum inundation under the same incident wave condition, i.e. the same ratio of wave height to water depth (a/h), the scour depth was the greatest

when the cylinder was placed at the onshore location when $a/h = 0.13$ or 0.05. On the other hand, the maximum scour depth occurred for the cylinder on the shoreline if the incident wave is $a/h = 0.09$, i.e. Case 5. In Case 5, breaking of the incident wave occurred and plunged just in front of the cylinder. Perhaps, this is the reason why the maximum scour occurred when the cylinder at the shoreline.

Figure 9 shows scour-depth variations (normalized by the cylinder diameter) at the side point of the cylinder wall. During the tsunami runup, scouring occurred in all cases. During the tsunami drawdown, sand deposition occurred in Cases 1, 2, and 3 in which the scour depth at the maximum inundation was large; on the other hand, further scouring occurred in the other cases. Comparing Fig. 9 with Fig. 8, scouring during the runup process is greater at the side of the cylinder than that at the point facing offshore. For the cases with the same incident wave condition, a/h, the scour depth at the maximum inundation is the greatest when the cylinder is placed offshore for $a/h = 0.13$ and 0.05. (Note that the maximum scour depths at the offshore side of the cylinder resulted when the cylinder was placed inshore as discussed with Fig. 8.) On the other hand, with $a/h = 0.09$, the largest scour at the maximum inundation occurred when the cylinder was placed at the shoreline. Again, wave breaking near the shoreline must be the reason for the case of $a/h = 0.09$.

Figure 10 shows scour-depth variations at the point facing in the onshore direction (behind the cylinder). On the contrary to the offshore and the side points presented in Figs. 8 and 9, sands were deposited behind the cylinder in most cases during the tsunami runup. During the tsunami drawdown, severe scouring occurred in most cases. Scour depths after the tsunami drawdown were as large as that of the side point at the maximum inundation stage shown in Fig. 9. For a given incident wave condition, scour depths after the tsunami drawdown were the greatest in the cases where the cylinder was on the shoreline, and the least in the cases where the cylinder was placed at the onshore location.

5. RELATION BETWEEN SCOUR DEPTH AND WAVE HEIGHT AND RUNUP WATER VOLUME

Figure 11 shows correlation coefficients between wave height and scour depth: the wave heights are those measured with the wave gages at seven different points (see Fig. 1) and the scour depths are those at the three points around the cylinder during tsunami runup and tsunami drawdown. At ① in Case 2 and Case 5, and at ①, ②, ③ and ④ in Case 3, the maximum wave height was set at 60 cm for the purpose of calculation for correlation coefficients because the water levels there became higher than the wave gage range of 60 cm.

During the tsunami runup, the scour depths at the point at the cylinder facing offshore have direct correlation to the wave heights at H_2, little to H_3 and ①. The scour depth at the side point of the cylinder during tsunami runup had positive correlation to the wave height at all points.

Unlike during the tsunami runup, the scour depth at the point of the cylinder facing offshore had inverse correlation only to H_3 during the tsunami drawdown. The scour depth at the side point of the cylinder during tsunami drawdown have direct correlation to the wave height at all points, particularly offshore points.

The water volume, which passed the cross section at 3 m offshore from the cylinder during the runup and drawdown, was calculated with following:

$$V_{in} = \int hu\,dt \quad (u>0) \qquad (1)$$

$$V_{out} = -\int hu\,dt \quad (u<0) \qquad (2)$$

where V_{in} is the total water volume per unit width during the flow in the onshore direction, V_{out} is the total water volume per unit width during the flow in the offshore direction, h is the local water depth and u is the horizontal velocity. Table 2 shows the correlation coefficients between the water volume and the scour depth at each point. V_{in} had little correlation with the scour depth at the point of the

cylinder wall facing offshore during tsunami runup, but had obvious correlation to that at the side point of the cylinder wall during tsunami runup, and at the side point and the onshore point during tsunami drawdown. Relation between V_{in} and scour depth at the onshore point during tsunami drawdown is shown in Figure 12. It indicates that there is a possibility of scour depth prediction at the side point and the onshore point with water volume of tsunami runup.

6. RELATION BETWEEN PORE PRESSURE AND SCOUR PROCESS

Soil liquefaction in seabed is often caused by a time lag between the pore pressure variation in the soil and the water pressure variation on the bed. By following the expression used by Zen (1987), vertical effective stress σ'_v can be expressed as

$$\sigma'_v = \sigma'_{v0} + (p_b - p_m) \qquad (3)$$

where σ'_{v0} is the initial vertical effective stress, p_b is the water pressure variation on the bed, p_m is the pore pressure variation. In this study, water pressure variations on the bed are approximated by the assumption of hydrostatic pressure.

Figures 13 and 14 show the temporal variations of water depth, pore pressure and vertical effective stress at 10 cm deep at ① shown in Figure 1, for Cases 2 and 3, respectively. Note that the water depth reached higher than 100 cm in Case 3 as shown in Fig. 14. Since the wave gage can measure only up to 100 cm, we simply set the depth at 100 cm during the period of overshoot. Since the duration of overshoot is short (less than 1 sec.), we feel that this error associated with the overshoot will not cause significant discrepancies in terms of the interpretations of our results. Compared between Figs. 13 and 14, the vertical effective stress is smaller in case 3 (the cylinder was at the offshore location) than in Case 2 (the cylinder was on the shoreline). As shown in Figure 8, however, the scour depth at the offshore side of the cylinder at the maximum inundation stage was less in Case 3 than in Case 2.

Figures 15 and 16 show temporal variations of water depth, pore pressure and vertical effective stress at 10 cm deep at ② and ③ (see Figure 1), for Cases 2 and 3, respectively. In comparison with ③, the water depth at ② was greater just after the tsunami arrival and lower after its quick decrease during the tsunami drawdown in both cases. The pore pressure at ② was as large as that at ③ during tsunami runup for Case 3, but during the drawdown, it was larger at ② than at ③ in both cases. At ②, the vertical effective stress was smaller throughout the tsunami runup and drawdown processes, and was zero in a longer period. These indicate that the decrease in vertical effective stress at the side of the cylinder was caused by the rapid water-depth decrease during the runup process and by water depth fall and delay of pore pressure fall in drawdown process.

7. CONCLUSION

The principal findings may be summarized as follows:

(1) Area and volume of scour are proportional to wave height. They are also dependent on the relative location of a cylinder to shoreline.

(2) The scour depth changed dynamically in runup and drawdown process. Instantaneous maximum scour depth reached five times as large as scour depth measured after the tsunami drawdown.

(3) In seabed near a cylinder, effective stress decreased notably during tsunami runup.

REFERENCES

Nishimura H., K. Horikawa (1979) : Scouring at the toe of a seawall due to tsunami drawdown, Proceedings of the 25th coastal engineering conference, pp. 210-214. (in Japanese)

Noguchi K., S. Sato and S. Tanaka (1997) : Large-scale experiments on wave overtopping and scouring at the toe of seawall, Proceedings of coastal engineering, vol. 44, pp. 296-300. (in Japanese)

Uda, T., A. Omata and Y. Yokoyama (1987) : Report of experiments on tsunami runup, Technical Memorandum of PWRI, No. 2486, 122 p. (in Japanese)
Zen, K., H. Yamazaki and A. Watanabe (1987) : Wave-induced liquefaction and densification in seabed, Report of the Port and Harbor Research Institute, vol. 26, No. 4, pp. 125-180. (in Japanese)

Table 1 Experiment condition

Case	WaterDepth(m)	WaveHeight(m)	a/h	RunupHeight(m)	
1	2.25	0.29	0.13	0.695	
2	2.45	0.32	0.13	0.755	
3	2.65	0.34	0.13	0.765	
4	2.25	0.20	0.09	0.580	
5	2.45	0.22	0.09	0.610	
6	2.65	0.24	0.09	0.650	
7	2.25	0.11	0.05	0.420	
8	2.45	0.12	0.05	0.435	
9	2.65	0.13	0.05	0.465	
10	2.65	0.24	0.09	0.670	no cylinder
11	2.45	0.22	0.09	0.660	no cylinder

Table 2 Correlation between water volume onshore and offshore, and scour depth

	offshore point		side point		onshore point	
	runup	drawdown	runup	drawdown	runup	drawdown
onshore water volume	0.16	0.01	0.54	0.23	0.24	0.81
offshore water volume	0.04	0.08	0.64	0.24	0.31	0.65

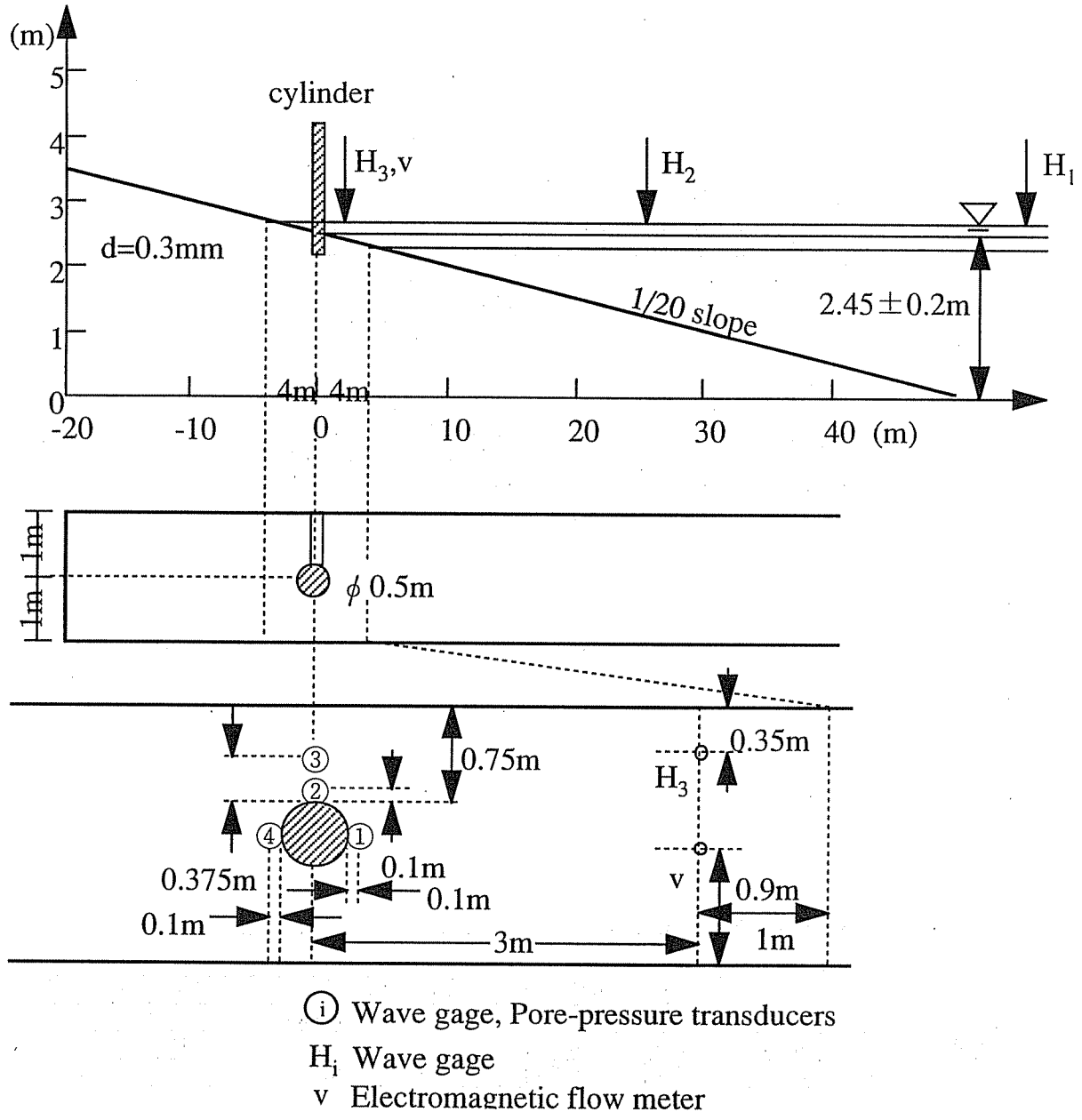

Figure 1 Experiment model

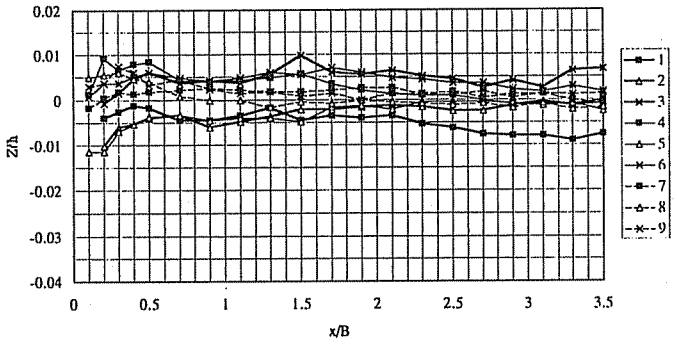

Figure 2 Seabed level variation on the offshore line from the cylinder

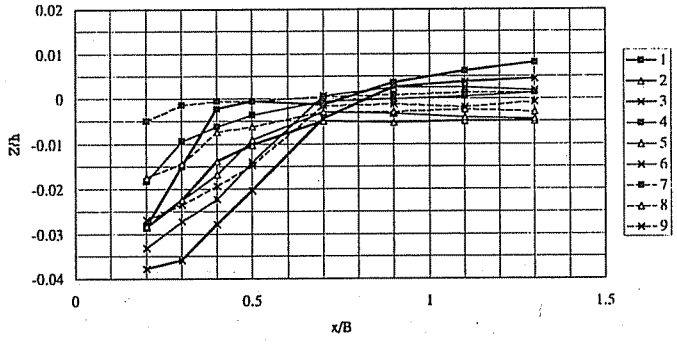

Figure 3 Seabed level variation on the longshore line from the cylinder

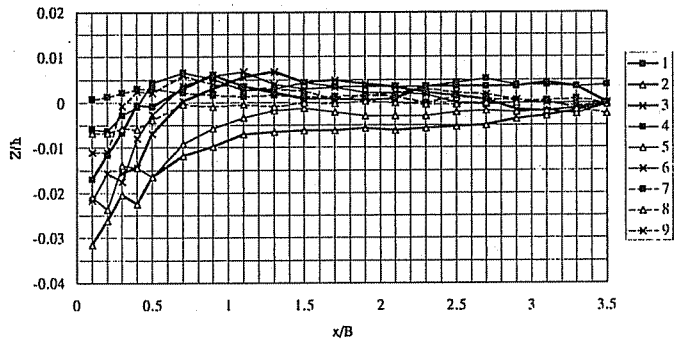

Figure 4 Seabed level variation on the onshore line from the cylinder

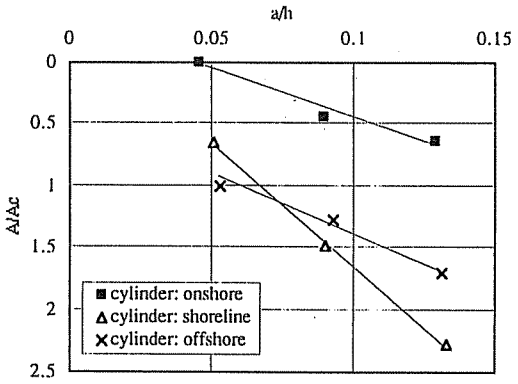

Figure 5 Wave height and scour area

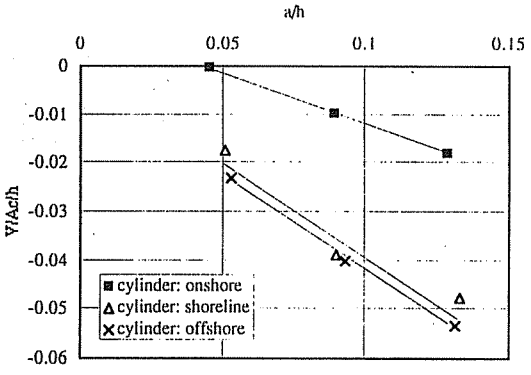

Figure 6 Wave height and scour volume

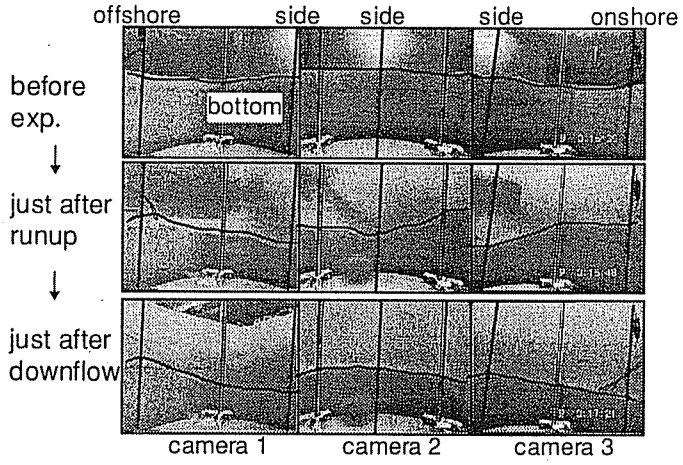

Figure 7 Scouring around the cylinder (case 3)

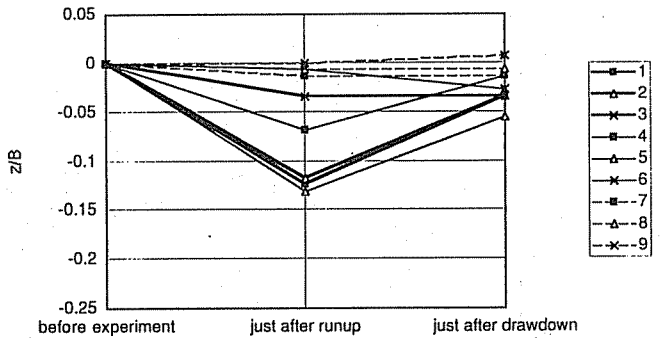

Figure 8 Scour depth at the offshore point

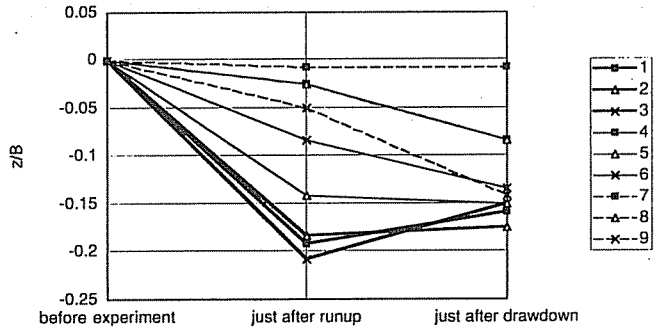

Figure 9 Scour depth at the side point

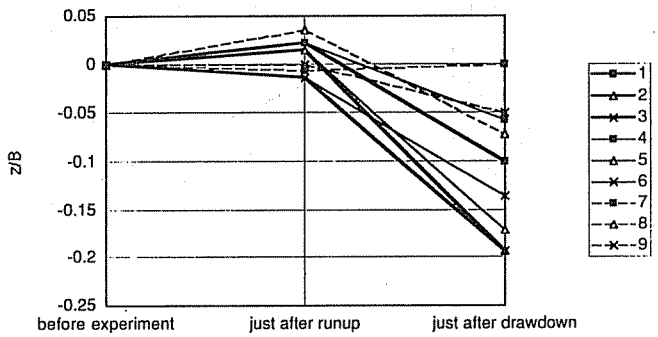

Figure 10 Scour depth at the onshore point

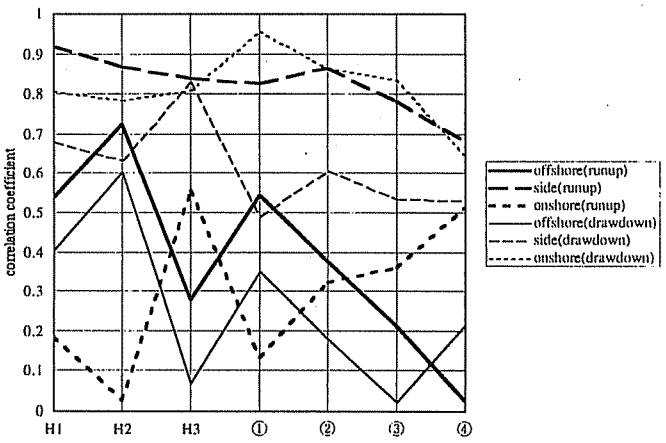

Figure 11 Correlation between wave height and scour depth

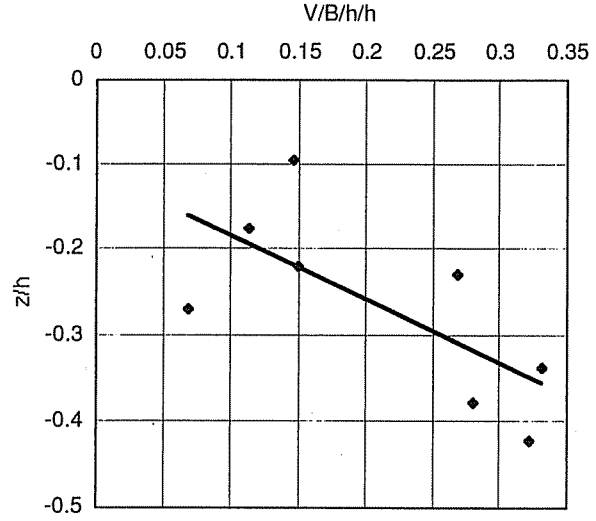

Figure 12 Onshore water volume and scour depth at the onshore point during tsunami drawdown

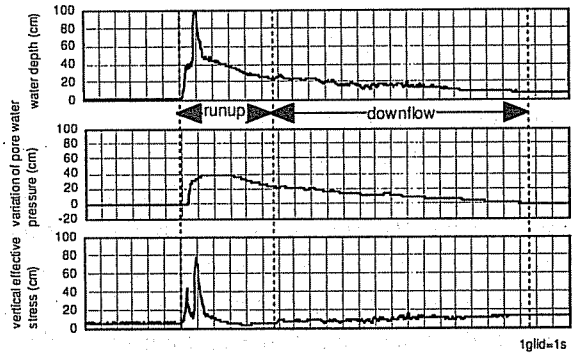

Figure 13 Water depth, pore pressure variation and vertical effective stress at the offshore point (case 2)

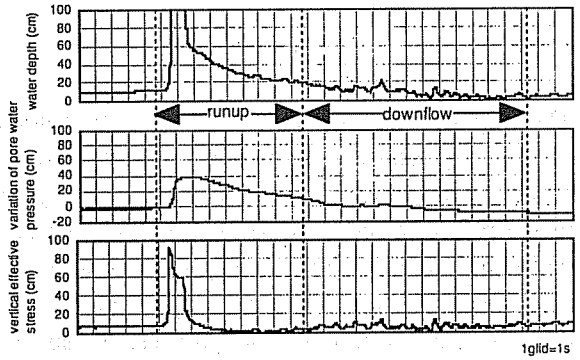

Figure 14 Water depth, pore pressure variation and vertical effective stress at the offshore point (case 3)

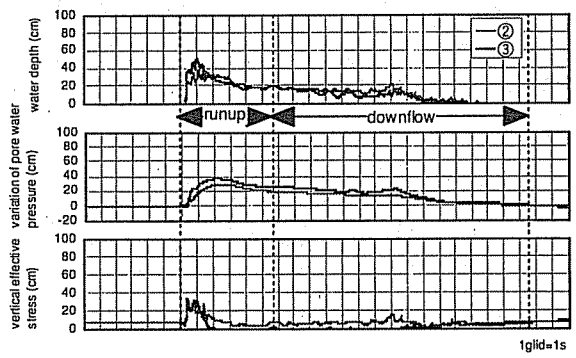

Figure 15 Water depth, pore pressure variation and vertical effective stress at the side point (case 2)

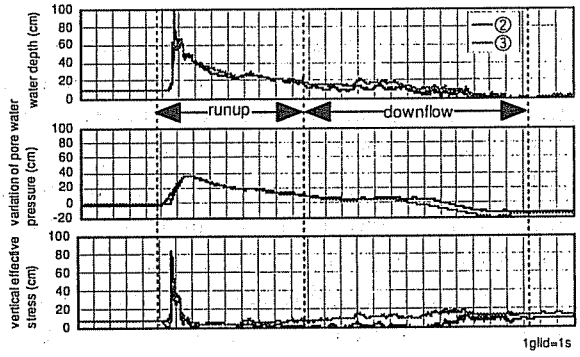

Figure 16 Water depth, pore pressure variation and vertical effective stress at the side point (case 3)